Electronic Structures of 9,10-Anthrylene Dimers and Trimers in Solution: Formation of Charge Separation States Depending on Alkyl Substituent Groups

Katsura Nishiyama,[†,⊥] Tsuyoshi Honda,[†] Heribert Reis,[‡,||] Uwe Müller,[§] Klaus Müllen,[§] Wolfram Baumann,*[,‡] and Tadashi Okada*[,†]

Department of Chemistry, Graduate School of Engineering Science and Research Center for Materials Science at Extreme Conditions, Osaka University, Toyonaka, Osaka 560, Japan; Institut für Physikalische Chemie, Universität Mainz, D-55099 Mainz, Germany; and Max-Planck-Institut für Polymerforschung, Ackermannweg 10, D-55128 Mainz, Germany

Received: October 7, 1997; In Final Form: December 31, 1997

Electronic structures of 9,10-anthrylene dimers and trimers analogous to 9,9′-bianthryl (BA) have been investigated by means of steady-state fluorescence and transient absorption spectroscopy and dipole moment evaluation based on the solvatochromic fluorescence shifts and integrated electrooptical emission measurements (IEOEM) in various solvents. Formation of the charge-separation (CS) state in the excited state was strongly dependent on the substituent group: unsubstituted and *n*-hexyl-substituted anthrylenes exhibited almost the same behavior compared to BA, whereas the *tert*-butyl-substituted dimer and trimer relaxed into an excitonic state rather than the CS state even in a polar solvent. The lower possibility of the CS state for the *tert*-butyl-substituted anthrylenes was mainly ascribed to the smaller solvation energy because of the larger effective Onsager cavity due to bulky *tert*-butyl groups. The limitation of a simple continuum model using Onsager's reaction field was also discussed in relation to the solvent-induced electronic structure change in the excited state of anthrylenes.

1. Introduction

The mechanism of the intramolecular charge-separation (CS) process for 9,9′-bianthryl (BA) has been a controversial issue with respect to its solvent-induced electronic structure change,[1−9] related within the framework of the "twisted intramolecular charge transfer" (TICT) state. In nonpolar solvents, both the fluorescence and $S_n \leftarrow S_1$ absorption spectra of BA are structured but broader than their corresponding spectra of anthracene, which has been attributed to the excitonic interaction between the two anthryl moieties.[10] With the increase of the solvent polarity, the contribution of the CS character to the excited electronic state is enhanced due to the solute−solvent interaction accordingly. The largely red-shifted, Gaussian-like fluorescence spectra in high polarity solvents are attributed mainly to the solvent-induced CS state. In the equilibrated excited state, it is believed that in polar solvents the energetically preferred CS state may be predominant, while the excitonic state is dominating in nonpolar solvents. Baumann et al. investigated the dipole moment of BA in the excited state in nonpolar-to-medium polarity solvents by means of integrated electrooptical emission measurements (IEOEM) and another method and also found that two different emitting states might be responsible for the excited state.[4] With respect to the characterization of the CS state of BA in the excited state in polar solvents, Mataga et al.[6] reported that the transient absorption spectrum of BA in acetonitrile could not be reconstructed as a superposition of the absorption spectra of the cation and anion radicals of anthracene, and they assigned the equilibrated excited state of BA in acetonitrile to a partial CS state, instead of the full electron transfer between the chromophores.

Lots of investigations have also been devoted for BA derivatives which have functional groups substituted onto the skeleton of BA. Mataga et al.[6] estimated the formation time constant of the CS state (τ_{CS}) of 10-chlorobianthryl in 1-pentanol to be 140 ps, while $\tau_{CS} = 170$ ps for BA in the same solvent, and they attributed the faster τ_{CS} for 10-chlorobianthryl to the symmetry breaking of the solvation due to the chlorine substituent. On the other hand, the absorption spectra of the excitonic and CS states of 10-chlorobianthryl were essentially similar to the corresponding spectra of BA, apart from minor spectral shifts. Kang et al.[5] intended to compare 2,2′,3,3′,6,6′,7,7′-octamethylbianthryl (OMBA) to BA whether the intramolecular torsional relaxation around the single C−C bond connecting the anthrylenes would affect the dynamics in the excited state in solution. Although some experimental difficulties existed owing to the low solubility of OMBA in solvents, within their results from the time-resolved fluorescence measurements a remarkable difference regarding to the dynamics part compared to BA was not observed. However, they reported that steady-state fluorescence spectra of OMBA in various solvents including hexane and acetonitrile are similar to those of BA.

From the spectroscopic point of view, it should be common that the steady-state absorption or fluorescence spectra of alkyl-substituted polyacenes would not largely differ from the parent compound except marginal spectral broadenings or shifts. However, it is still ambiguous for BA and related compounds how the molecular and electronic structures of the monomeric anthracene subunit relate to the formation of the intramolecular

[†] Osaka University.
[‡] Universität Mainz.
[§] Max-Planck-Institut für Polymerforschung.
[⊥] Present address: Venture Business Laboratory, Osaka University, Suita, Osaka 565, Japan.
[||] Present address: Institute of Organic and Pharmaceutical Chemistry, National Hellenic Research Foundation, 48 Vas. Constantinou Ave., Athens 116 35, Greece.

S1089-5639(97)03251-9 CCC: $15.00
Published on Web 04/07/1998

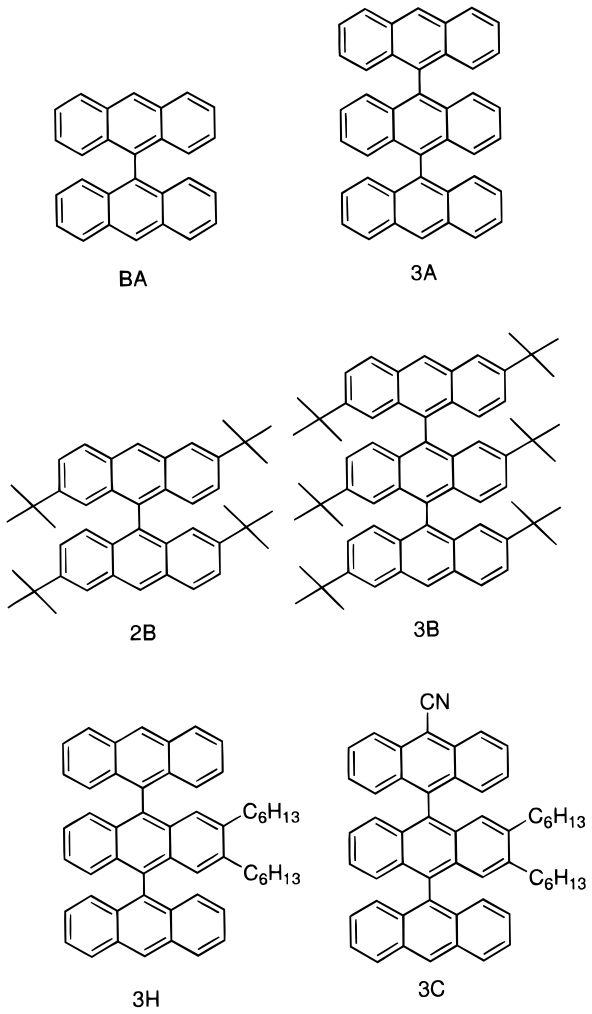

Figure 1. Anthrylene dimers and trimers investigated here.

CS state. In this paper the behavior of the excited state of trisanthryl 3A, its di-*n*-hexyl-substituted derivative 3H[11] as well as the *tert*-butyl-substituted analogues bianthryl 2B and trisanthryl 3B is compared to that of BA. The structures of the anthrylenes investigated here are given in Figure 1. Steady-state fluorescence and transient absorption spectroscopy in various solvents have been applied for the anthrylenes. Dipole moments in the excited state were determined by means of solvatochromic fluorescence peak shifts and IEOEM. Consistency between the results obtained from each experimental method will also be discussed.

2. Theoretical Backgrounds on Dipole Moments in the Excited State

Here let us pause to review the theoretical basis on experimentally observable dipole moments in solution. Within the context of Onsager's model, the permanent point dipole $\boldsymbol{\mu}^0$ of the solute molecule located at the center of an empty sphere with the radius a_0 polarizes surrounding solvent molecules.[12,13] The experimentally observable dipole moment $\boldsymbol{\mu}$ in a given state in solution can be expressed as the sum of the term of the permanent dipole $\boldsymbol{\mu}^0$ and the solvent-induced part through the reaction field $\boldsymbol{R}$:

$$\boldsymbol{\mu} = \boldsymbol{\mu}^0 + \alpha \boldsymbol{R} \tag{1}$$

with

$$\boldsymbol{R} = f\boldsymbol{\mu} \tag{2}$$

$$f = \frac{1}{4\pi\epsilon_0 {a_0}^3} \frac{2(\epsilon - 1)}{2\epsilon + 1} \tag{3}$$

where α is the polarizability of the solute molecule, ϵ_0 the permittivity of the vacuum, and ϵ the relative permittivity of the corresponding solvent. In this definition $\boldsymbol{\mu}^0$ can be interpreted as a dipole moment in the gas phase and it should be independent of the solvent polarity in the case of a sufficiently rigid molecule.

To determine a dipole moment in the equilibrated excited state $\boldsymbol{\mu}_e$, conventionally, a solvatochromic shift of the fluorescence peak wavenumber is recorded as a function of ϵ and the refractive index n of the solvent. Our final goal is to correlate the fluorescence Stokes shift to the solute dipole moments in the ground and equilibrated excited state $\boldsymbol{\mu}_e$ and $\boldsymbol{\mu}_g$, respectively. A brief outline behind this experimentally useful relation is surveyed here, which is well-known as the Mataga−Lippert equation.[14,15] In general, optical absorption and fluorescence spectra are given as the energy difference between the respective initial and final states. The energy in each state can be calculated to be the sum of the energy of the solute in the corresponding electronic state in the gas phase, the interaction energy between the dipole moment of the solute and the reaction field, and the energy to let surrounding solvent molecules polarized. The fluorescence Stokes shift can be expressed as the energy difference between the absorption and fluorescence maxima:[16]

$$hc(\tilde{\nu}_a - \tilde{\nu}_e) = \frac{1}{4\pi\epsilon_0} \frac{2({\boldsymbol{\mu}_e}^2 - \boldsymbol{\mu}_e \cdot {\boldsymbol{\mu}_g}^{FC} - \boldsymbol{\mu}_g \cdot {\boldsymbol{\mu}_e}^{FC} + {\boldsymbol{\mu}_g}^2)}{{a_0}^3} \times (f_\epsilon - f_n) + \frac{1}{4\pi\epsilon_0} \frac{({\boldsymbol{\mu}_e}^2 - ({\boldsymbol{\mu}_g}^{FC})^2 - ({\boldsymbol{\mu}_e}^{FC})^2 + {\boldsymbol{\mu}_g}^2)}{{a_0}^3} f_n \tag{4}$$

with

$$f_\epsilon = \frac{\epsilon - 1}{2\epsilon + 1}, \qquad f_n = \frac{n^2 - 1}{2n^2 + 1}$$

where $\tilde{\nu}_a$ and $\tilde{\nu}_e$ are the absorption and fluorescence maximum wavenumbers, respectively, ${\boldsymbol{\mu}_e}^{FC}$ and ${\boldsymbol{\mu}_g}^{FC}$ correspond to the solute dipole moments in the excited and ground Franck−Condon states, respectively, and h and c have usual meaning. It should be stressed here that all the dipole moments presented above, $\boldsymbol{\mu}_e$, $\boldsymbol{\mu}_g$, ${\boldsymbol{\mu}_e}^{FC}$, and ${\boldsymbol{\mu}_g}^{FC}$, correspond to $\boldsymbol{\mu}$ and not $\boldsymbol{\mu}^0$, within the notation of eq 1.

If it is assumed that the dipole moments in the excited and ground equilibrium states are equal to those in their corresponding Franck−Condon states, eq 4 can be expressed as

$$hc(\tilde{\nu}_a - \tilde{\nu}_e) = \frac{1}{4\pi\epsilon_0} \frac{2(\boldsymbol{\mu}_e - \boldsymbol{\mu}_g)^2}{{a_0}^3} (f_\epsilon - f_n) \tag{5}$$

For the particular case where a principal fluorescence solvatochromic shift is not detected in nonpolar solvents, but essential solvatochromic shifts are observed in higher polar solvents, it can be assumed that only $\boldsymbol{\mu}_e$ has a substantial value and the other dipole moments can be negligibly small. In such a case eq 4 can be reduced to[16]

$$hc(\tilde{\nu}_a - \tilde{\nu}_e) = \frac{1}{4\pi\epsilon_0}\frac{2|\boldsymbol{\mu}_e|^2}{{a_0}^3}\left(f_\epsilon - \frac{1}{2}f_n\right) \quad (6)$$

For an exciplex, or BA, one should not observe the absorption band that corresponds to the CS state in the ground state. Then eq 6 is further simplified as

$$hc\tilde{\nu}_e = \text{const} - \frac{1}{4\pi\epsilon_0}\frac{2|\boldsymbol{\mu}_e|^2}{{a_0}^3}\left(f_\epsilon - \frac{1}{2}f_n\right) \quad (7)$$

Based on eq 7, a plot of $\tilde{\nu}_e$ as a function of the solvent parameter $f_\epsilon - (1/2)f_n$ would yield a straight line, and the slope of the plot $(-1/4\pi\epsilon_0)(2|\boldsymbol{\mu}_e|/{a_0}^3)$ is a direct experimental observable from which $\boldsymbol{\mu}_e$ can be estimated under an appropriate assumption of a_0.

One of the other methods to determine $\boldsymbol{\mu}_e$ is IEOEM, utilizing the fluorescence anisotropy induced by an external electric field. Elaborated theoretical and experimental details have been described by Liptay[17] and Baumann.[13,18−20] Here the theoretical model is briefly surveyed. According to Onsager's model, under the influence of an externally applied electric field $\boldsymbol{E}_a$, the electric field inside the cavity $\boldsymbol{E}_i$ is related to $\boldsymbol{E}_a$ as

$$\boldsymbol{E}_i = g(\epsilon)\boldsymbol{E}_a \quad (8)$$

with

$$g(\epsilon) = \frac{3\epsilon}{2\epsilon + 1} \quad (9)$$

In a solute−solvent system, the energy of the system is considered to be distributed, reflecting the different degree of the orientational distribution of solvent molecules around the solute molecule. In the thermal equilibrium state without $\boldsymbol{E}_a$, we can assume that the distribution could be expressed by a Boltzmann distribution function. Under the application of $\boldsymbol{E}_a$ the energy distribution should be disturbed due to a scalar product of $\boldsymbol{E}_a \cdot \boldsymbol{\mu}_e$, which could bring about the intensity change of the polarized fluorescence at a given wavelength. Our interest is to relate this change to $\boldsymbol{\mu}_e$ of the solute molecule. This method is, in general, known as electrooptical emission measurements (EOEM). The photon current q emitted from the solution observed under $\boldsymbol{E}_a$ is expressed approximately as

$$q^{\boldsymbol{E}_a}(\phi,\tilde{\nu}) = q^{\boldsymbol{E}_a=0}(\phi,\tilde{\nu})[1 + X(\phi,\tilde{\nu})\boldsymbol{E}_a{}^2] \quad (10)$$

where ϕ is the angle between the electric field vector of the detecting linear polarized fluorescence which is to be analyzed and the external electric field. The quantity $X(\phi,\tilde{\nu})$ must be experimentally determined and could be related to the solute dipole moment in the excited state. In the present measurements, the photon current was integrated over a suitable emitting wavelength region in order to remarkably enhance the signal-to-noise ratio and to save long time measurements in order to prevent photochemical breakdown processes. This method is referred to as IEOEM: eq 10 can be reduced to

$$q^{\boldsymbol{E}_a}(\phi) = q^{\boldsymbol{E}_a=0}(\phi)[1 + X(\phi)\boldsymbol{E}_a{}^2] \quad (11)$$

$$X(\phi) \approx L(\chi) + ({}^eE/30)s(\phi) + \text{O(PM)} \quad (12)$$

where $L(\chi)$ describes the relative field-dependent intensity change of the ground-state absorption spectra with the angle χ between the excitation polarization and the external field. $s(\phi) = 3\cos^2\phi - 1$, and O(PM) is the small correction term related to the spectral characteristics of the photomultiplier observing the emission photon current and can be neglected. ${}^eE$ is the term related to the excited-state dipole moment and

$${}^eE = (1/k_BT)^2 g^2(\epsilon)[3(\boldsymbol{m}_e\cdot\boldsymbol{\mu}_e)^2 - \boldsymbol{\mu}_e{}^2] \quad (13)$$

where $\boldsymbol{m}_e$ denotes a unit vector of the direction of the transition moment, k_B the Boltzmann constant, T absolute temperature. $|\boldsymbol{\mu}_e|$ thus can be determined with at least two different values of $X(\phi)$: changing the angle of ϕ. For the anthrylene oligomers investigated here, $\boldsymbol{\mu}_e$ can be related as

$$X(\phi{=}0°) - 3X(\phi{=}90°) = g^2(\epsilon)\boldsymbol{\mu}_e^2/3(k_BT)^2 \quad (14)$$

assuming that the direction of the transition moment and that of the dipole moment in the excited state to be parallel.

3. Experimental Section

Steady-state absorption spectra were detected by using Shimadzu UV-260 and Hitachi 340 spectrometers. Corrected steady-state fluorescence spectra were observed by Hitachi 850E and Perkin-Elmer LS50B spectrophotometers. For picosecond transient absorption measurements, the second harmonics of the output of a dye laser (10 ps fwhm, 341−355 nm) excited by a second harmonics of a mode-locked Nd^{3+}:YAG laser was employed as an excitation light source.[21] All solutions were deaerated by a nitrogen gas stream before the measurements. Spectrograde solvents were used as received.

The same experimental setup for IEOEM was employed as was reported elsewhere.[4,13,18] The solution was excited by a high-pressure mercury lamp (500 W). The fluorescence photon current was detected by a photomultiplier placed on the perpendicular against the excitation axis. Since the resultant signal was so small, $X(\phi)$ was detected through a lock-in amplifier locked to the modulated field $\boldsymbol{E}_a$. The photon flux from the entire emission band of the solute was collected unless otherwise noticed, under the conditions of $X(0°)$ and $X(90°)$. In some measurements appropriate cutoff filters were used to observe a specific fluorescence wavelength region. $\boldsymbol{E}_a$ between the electrodes (5 mm) in the solution cell was typically 6.0×10^5 V m^{-1}.

Synthesis and purification of the compounds shown in Figure 1 were described elsewhere.[22] The purity of the compounds was verified by thin-layer chromatography and/or HPLC. The steady-state absorption and fluorescence spectra were also scrutinized to confirm that the impurity-originated spectral bands were not observed. For IEOEM, cyclohexane ($\epsilon = 2.0$) and dioxane ($\epsilon \approx 6$ as microscopic relative permittivity[13]) were carefully distilled immediately before the measurements. Trifluorotoluene ($\epsilon = 9.0$) was purified by an alumina column chromatography. To avoid electrical breakdown of the solution, special care was also taken to reduce the water in the solution. All measurements have been carried out at room temperature (22 °C) unless otherwise described.

4. Results

Solvent Effects on Steady-State Absorption and Fluorescence Spectra. The steady-state absorption spectra of the anthrylenes in cyclohexane and the fluorescence spectra in various solvents at room temperature are depicted in Figure 2. The absorption spectra studied here are essentially independent of the solvents used. For **BA**, the fluorescence spectrum in the nonpolar solvent is structured but broader than that of an-

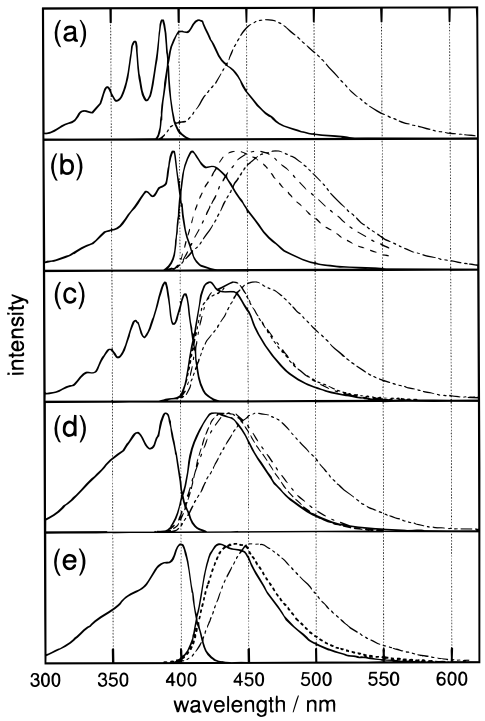

Figure 2. Steady-state absorption spectra and fluorescence spectra in various solvents of **BA** (a), **3A** (b), **3H** (c), **2B** (d), and **3B** (e) at room temperature. The solvents are cyclohexane (solid line), diethyl ether (dotted line), dioxane (dashed line), trifluorotoluene (dot−dashed line), and DMF (dot−dot−dashed line).

thracene, which has been assigned to be the emission from the excitonic state. With the increase of the solvent polarity, the fluorescence spectrum of **BA** shifts toward the red and becomes more structureless, which has been ascribed to the formation of the CS state. In the case of the present compounds, for **3A** and **3H**, the spectral behavior is very similar to that of **BA**. In cyclohexane, the structured fluorescence spectra of **3A** and **3H** are similar to that of **BA**. In polar solvents, a large Stokes shift was observed for **3A** likewise **BA**. Though the fluorescence spectra of **3H** in polar solvents may seem to indicate a smaller solvatochromic peak shift compared to **BA** and **3A**, however, a spectral decomposition method was proven to work sufficiently.[11] As a result, for **3H** the CS emission maximum was assigned to be 472 nm in *N*,*N*-dimethylformamide (DMF), for example, whose solvatochromic shift was rather comparable to that of **BA** or **3A**. On the other hand, the situation for the *tert*-butyl-substituted **2B** and **3B** seems to be different. The absorption spectra of **2B** and **3B** are much more broadened compared to those of other anthrylenes. The fluorescence Stokes shift in polar solvents were also observed; however, the red shifts were much smaller. It is implied that the electronic structure in the excited state in polar solvents of **2B** and **3B** differs from those of **BA**, **3A**, and **3H**. We also measured the steady-state absorption and fluorescence spectra of 2,3-dihexylanthracene and 2,6-di-*tert*-butylanthracene. The absorption and fluorescence spectra of the compounds are very similar to each other and show marginal broadening and spectral shifts compared to anthracene or **BA**. Both the *n*-hexyl and *tert*-butyl substituents would not largely perturb the electronic structure of anthracene.

Figure 3 illustrates the representatives of solvatochromic shifts of the fluorescence spectral peak recorded in various solvents with the bulk polarity, solvents used are given in the figure caption. In Figure 3, the plot for **3B** in a nonpolar solvent cyclohexane remarkably shifts toward the red compared with

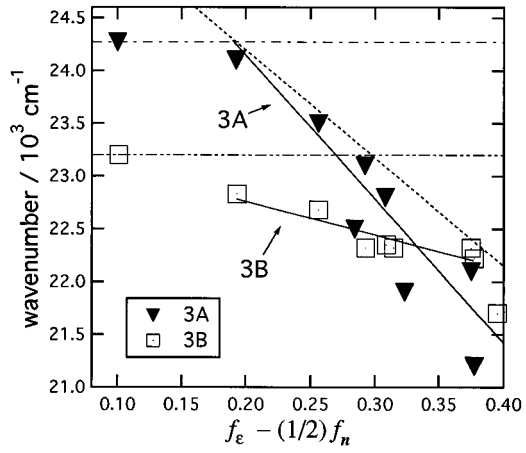

Figure 3. Fluorescence maxima of **3A** (triangles) and **3B** (squares) plotted against the solvent parameter $f_\epsilon - (1/2)f_n$ according to eq 7. The solvents given are cyclohexane ($f_\epsilon - (1/2)f_n = 0.119$), butyl ether (0.192), diethyl ether (0.256), dioxane (0.284, where $\epsilon \approx 6$ as the microscopic relative permittivity was used[13]), ethyl acetate (0.293), tetrahydrofuran (0.307), dichloromethane (0.315), trifluorotoluene (0.323), acetone (0.375), *N*,*N*-dimethylformamide (0.378), *N*-methylformamide (0.395). The solid lines correspond to the averaged slope of the plots obtained in polar solvents, from which the value of $\boldsymbol{\mu}_e$ was calculated according to the Mataga−Lippert equation (eq 7). The dotted line shows an estimated energy of the CS state of **3B** with dipole moment of 21 D. The dot−dashed and dot−dot−dashed lines indicate the energy of the excitonic fluorescence of **3A** and **3B**, respectively. See the Discussion for details.

TABLE 1: Dipole Moments in the Excited State Obtained from the Solvatochromic Plots

compounds	a_0/Å[a]	$\boldsymbol{\mu}_e$/D[a]	a_0/Å[b]	$\boldsymbol{\mu}_e$/D[b]
BA	6	20	6	20
3A	9	31	6.8	21
3H	9	35	7.5	27
2B	6	12	7.0	15
3B	9	16	7.5	12
3C	9	32	7.7	25

[a] Cavity radii a_0 for the anthrylenes that cover the entire molecules (6 Å for dimers and 9 Å for trimers), from which $\boldsymbol{\mu}_e$ were estimated based on eq 7. [b] Cavity radii a_0 derived from an empirical molecular weight model, where $a_0(i) = \sqrt[3]{M_w(i)/M_w(\mathrm{BA})}\,a_0(\mathbf{BA})$, with M_w the molecular weight of the solute molecule *i*, *i* denotes anthrylenes, and $a_0(\mathbf{BA}) = 6$ Å was assumed.

that of **3A**. This can be explained by the red shift of the 0−0 transition band as seen obviously from Figure 2. The solid lines show the averaged slope of the plot determined from the region 0.20−0.38 of the abscissa, from which the value of $\boldsymbol{\mu}_e$ was calculated according to the Mataga−Lippert equation (eq 7). In nonpolar solvents, the fluorescence from the excitonic state can be predominant, which gives rise to the deviation of the plots from the straight line at the left end of the graph. Table 1 compares $\boldsymbol{\mu}_e$ estimated from the Mataga−Lippert relation using the observed slopes. To calculate $\boldsymbol{\mu}_e$, (i) a_0 was assumed as a sphere which covers the molecule, 6 Å for dimers and 9 Å for trimers; (ii) according to an empirical model where the cavity is considered to be proportional to the third root of the molecular weight, in which $a_0 = 6$ Å for **BA** was assumed. In these cases the latter estimation results in a milder increase of a_0 except **2B**. According to eq 7, the calculation of the absolute value of $\boldsymbol{\mu}_e$ depends on the parameter a_0 to the $^3/_2$ power; however, the relative values are independent of the calculation details. Table 1 actually shows that smaller $\boldsymbol{\mu}_e$ are especially obtained for **2B** and **3B**, corresponding to the smaller fluorescence Stokes shifts in polar solvents.

TABLE 2: Experimental Results Derived from IEOEM

	μ_e/D[a]					
	cyclohexane	dioxane	trifluorotoluene	$\alpha/a_0^3/10^{-10}$ C V^{-1} m^{-1} [b]	$\alpha'/10^{-24}$ cm^3 [c]	$\alpha'/10^{-24}$ cm^3 [d]
BA[e]	3.0	7.4		1.14	220	220
3A	3.1	6.5	9.8	0.99	650	280
3H	4.2	6.7	9.0	0.93	610	350
2B	3.1	4.9	7.2	0.90	180	280
3B	3.7	4.5	6.5	0.80	520	300
3C	16.6	17.4	24.3	0.65	430	270

[a] Solvent dependences of dipole moments in the excited state. Solvents used are given in the table. [b] Polarizability densities of the anthrylenes in the excited state estimated by the relation between $1/|\boldsymbol{\mu}_e|$ and the function of the solvent polarity, as given in eq 15. Note that in this estimation it is assumed that the entire part of the solvent dependence of $\boldsymbol{\mu}_e$ is attributed to the induced part of the dipole moment arisen from the term $\alpha\boldsymbol{R}$ within the description of eq 1. [c] Polarizability volumes α' ($=\alpha/4\pi\epsilon_0$) calculated with a_0 where $a_0 = 6$ Å was assumed for dimers and 9 Å for trimers. [d] Polarizability volumes α' ($=\alpha/4\pi\epsilon_0$) calculated with a_0 derived from the empirical molecular weight model. See Table 1 for each value of a_0. [e] The data of **BA** are taken from ref 4.

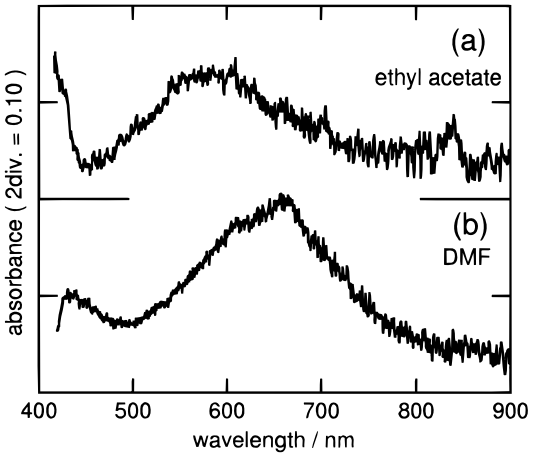

Figure 4. Solvent dependences of the transient absorption spectra of **3A** detected at 100 ps after the laser excitation at room temperature. Solvents used are ethyl acetate (a) and DMF (b). Note that the transient absorption spectra of **3A** in nonpolar solvents could not be detected owing to poor solubility.

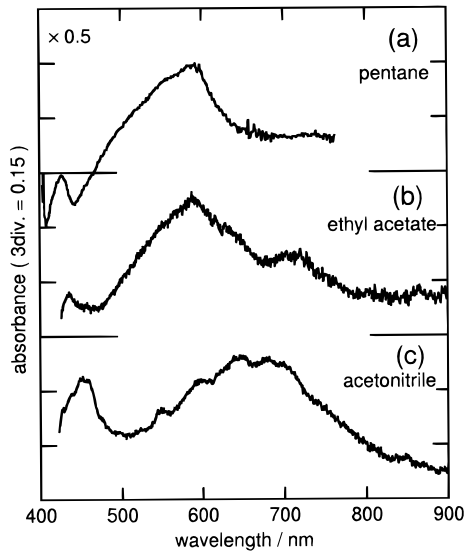

Figure 5. Solvent dependences of the transient absorption spectra of 3H detected at 100 ps after the laser excitation at room temperature. Solvents used are pentane (a), ethyl acetate (b), and acetonitrile (c).

Dipole Moments Obtained by Means of IEOEM. Solvent dependencies of the dipole moments of the anthrylenes in the excited state determined from IEOEM based on eq 14 are summarized in Table 2. In the present measurements the term $L(\chi)$ in eq 12 can be neglected because the anthrylene oligomers investigated here do not have substantial dipole moments in their ground states. It was actually proven that experimentally obtained $L(\chi)$ values affect $\boldsymbol{\mu}_e$ by 0.3% for **3H** and <0.1% for **3B**, respectively. In the nonpolar solvent cyclohexane, the nonvanishing dipole moments were estimated by this method for the compounds. For all the anthrylenes, $\boldsymbol{\mu}_e$ increases with the solvent polarity, where $\boldsymbol{\mu}_e$ for **2B** and **3B** in dioxane and trifluorotoluene are much smaller than those of any other substances in the corresponding solvent. The lower contribution of the formation of the CS state of **2B** and **3B** is therefore implied by IEOEM, which is fully consistent with relatively smaller $\boldsymbol{\mu}_e$ for **2B** and **3B** from the solvatochromic plot, corresponding to a small Stokes shift of **2B** and **3B** even in polar solvents. Instead of the qualitative consistency of $\boldsymbol{\mu}_e$, however, discrepancies between the absolute values of $\boldsymbol{\mu}_e$ detected from the solvatochromic plots and those from IEOEM were recognized. This point will be further discussed in the later section.

Solvent Effects on Transient Absorption Spectra. Figures 4−7 display transient absorption spectra of the anthrylenes in various solvents. The spectra shown in Figures 4−7 were detected at 100 ps after the excitation. Evolution of spectra with time was precisely recorded from just after the excitation up to 6 ns, and essential spectral changes were not detected within the time resolution of the apparatus used (10 ps), except the intensity decay of the absorbance due to the population decay with the lifetime of the excited state (>5 ns, depending on the solvent). In addition, according to the literature the mean solvation time $\langle\tau_s\rangle$ was estimated to be 2.7 ps in ethyl acetate[23] and 0.26 ps in acetonitrile,[24] for example, based on time-resolved Stokes shift measurements. Hence we assign the absorption spectra shown in Figures 4−7 from the respective equilibrated excited states. The negative depressions in the shorter wavelength regions observed particularly in nonpolar solvents are ascribed to the induced fluorescence, and they are in agreement with their fluorescence spectra.

For **BA**[7] and **3H**[11] we found that in the nonpolar glass matrix of MP (methylcyclohexane and isopentane mixed) at 77 K the transient absorption spectra were essentially corresponding to anthracene or 2,3-dihexylanthracene.[11] At room temperature in the nonpolar fluid solvent, the transient absorption spectra of **BA**[7] and **3H** (Figure 5) were more structureless compared with those in a glass matrix (and the $S_n \leftarrow S_1$ absorption spectra of their monomers at room temperature), which were assigned to be the excitonic interaction between the chromophores. The anthryl moieties are thus assumed to be perpendicular in the ground state, but they are twisted in the relaxed excitonic state, which is also suggested by the behavior of the steady-state fluorescence spectra.[7,11] Acquisition of the transient absorption spectra of **3A** in a nonpolar solvent was not possible because

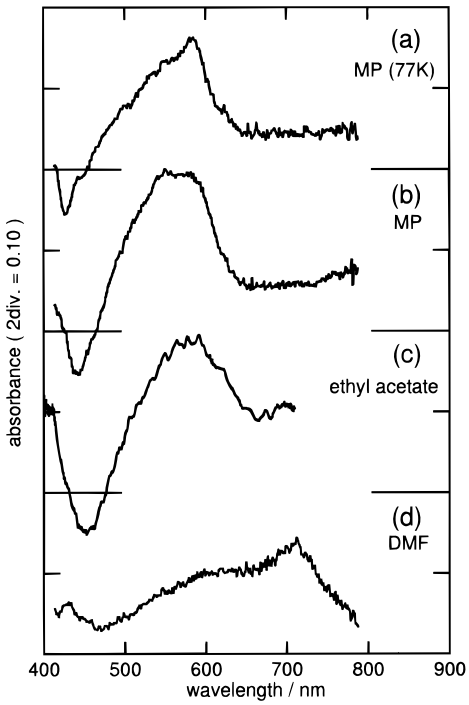

Figure 6. Solvent dependences of the transient absorption spectra of **2B** detected at 100 ps after the laser excitation. Solvents used are the nonpolar glass matrix of "MP" (methylcyclohexane and isopentane mixed) at 77 K (a), the fluid nonpolar solvent MP (b), ethyl acetate (c), and DMF (d). The measurements were performed at room temperature except (a).

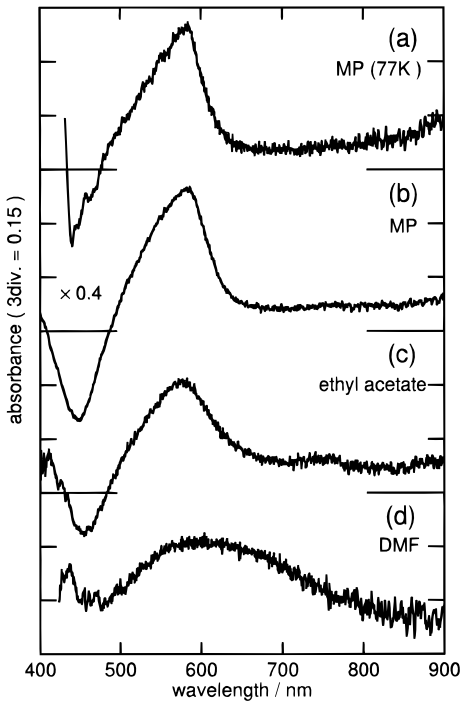

Figure 7. Solvent dependencies of the transient absorption spectra of **3B** detected at 100 ps after the laser excitation. Solvents used are MP at 77 K (a), MP (b), ethyl acetate (c), and DMF (d). The measurements were performed at room temperature except (a). Refer also the caption of Figure 6 for the abbreviation of MP.

of the low solubility of the compound. However, as mentioned above, the steady-state fluorescence spectrum of **3A** in the nonpolar solvent corresponds to that of **BA** and **3H**. Thus it could be assumed that **3A** also should form a similar excitonic state likewise **BA** and **3H** in the nonpolar solvent. For **2B** (Figure 6) and **3B** (Figure 7) the detected spectra in the glass matrix at 77 K have rather sharp spectral maxima around 590 nm, and they are essentially equal to the $S_n \leftarrow S_1$ absorption spectrum of 2,6-di-*tert*-butylanthracene at room temperature, as shown in Figure 8a. On the other hand, at room temperature the transient spectra are broader and more structureless compared to those detected in the glass matrix. The spectral behavior of **2B** and **3B** in a nonpolar solvent is similar to that of **BA** or **3H**.

We next discuss the transient absorption spectra in medium polar and polar solvents. The transient absorption spectra of **3A** in DMF (Figure 4b) and **3H** in acetonitrile (Figure 5c) in their equilibrated excited states are practically the same as that of **BA** in acetonitrile. The broad absorption bands with maxima around 680 nm that are not observed in the nonpolar solvent can be attributed to the CS state absorption. It can be noted here that the transient absorption spectra of **3A** and **3H** in polar solvents could not be reproduced as a superposition of the absorption band of the cationic and anionic species of their corresponding anthrylene subunits, and the CS state of **3A** or **3H** in polar solvents should be assigned to a partial CS state and not to a full electron-transfer state between the chromophores, like in the case of **BA**.[7] In the medium polar solvent ethyl acetate with $\epsilon \approx 6.1$, corresponding to ϵ of dioxane which was used as one of the solvents in our present IEOEM, the broader absorption band around 700 nm for **3H** (Figure 5b) which is not recognized in the nonpolar solvent is attributed to the contribution from the CS state. For **3A** in ethyl acetate (Figure 4a), the spectrum is broader than that of **BA** or **3H** in

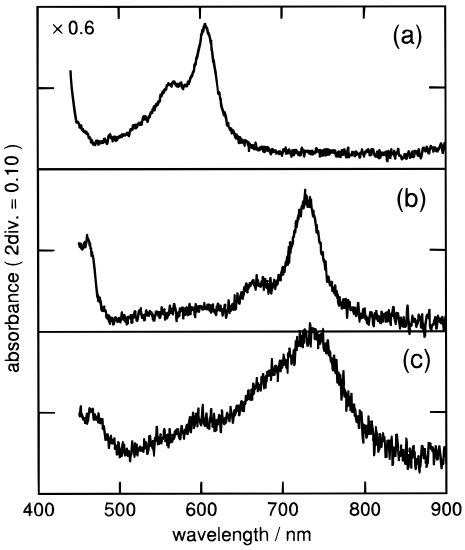

Figure 8. $S_n \leftarrow S_1$ absorption spectra of 2,6-di-*tert*-butylanthracene in cyclohexane (a). Also shown are the absorption spectra of cation (b) and anion (c) radical bands of 2,6-di-*tert*-butylanthracene in acetonitrile solution, obtained by adding 1,2,4,5-tetracyanobenzene (TCNB) (b) and *N*,*N*-dimethylaniline (DMA) (c), respectively. For the ionic absorption spectra, the absorption bands in the wavelength region shorter than 500 nm are mainly ascribed to the TCNB anion (b) and DMA cation (c) bands.

nonpolar solvents, and it shows substantial contribution still in the wavelength region longer than 650 nm, both of which are ascribed to emergence of the CS state to some extent. However, for **3A** in ethyl acetate, relative contribution from the CS state to the spectrum is lower compared with the case of **3H** in the same solvent (Figure 5b), and the entire spectral shape may instead be rich in contribution from the excitonic state. It should be mentioned here that the transient absorption spectrum of **3H**

in ethyl acetate was proven to be reconstructed approximately as a superposition of the transient absorption spectra of **3H** in the nonpolar solvent and that in the polar solvent (acetonitrile), as was the case of **BA**.[25] For **3A**, although transient absorption spectroscopy in nonpolar solvents was not available as described above, the transient absorption spectrum of **3A** in ethyl acetate can also be approximately expressed as the summation of the transient spectra of **BA** in the nonpolar solvent and that of **3A** in the polar solvent. As the result, the solvent dependence of the transient absorption spectra observed here can be ascribed to the substantial change of the electronic state of the solute, which is induced by the solute−solvent interaction.

On the other hand, the transient absorption spectra of *tert*-butyl-substituted **2B** and **3B** in the polar and medium polar solvents, as seen from Figures 6c,d, and 7c,d, are much different from those of **BA**, **3A**, and **3H**. The absorption spectra of the 2,6-di-*tert*-butylanthracene cation and anion radicals are also depicted in Figure 8b,c. In the polar solvent DMF, the obtained spectra for **2B** and **3B** could not be reconstructed as the summation of the cationic and anionic radical absorption bands of 2,6-di-*tert*-butylanthracene. The additional absorption bands in DMF around 700−800 nm which were not detected in the nonpolar solvent implies that **2B** and **3B** could achieve the CS state to some extent: however, the entire spectral shapes for **3B** in DMF and, even more, in ethyl acetate are rather closer to the excitonic state observed in the nonpolar solvent. The transient absorption spectrum of **2B** in DMF is also different from those of **BA**, **3A**, and **3H** in the polar solvent. At any rate, the result obtained from the transient absorption spectroscopy is qualitatively consistent with the smaller Stokes shifts and $\boldsymbol{\mu}_e$ for **2B** and **3B** as mentioned in the previous section.

5. Discussion

Interpretation of the Solvent-Induced Electronic Structure Change and Experimentally Observed Dipole Moments. Discrepancy of absolute values of $\boldsymbol{\mu}_e$ has been observed between those detected from the solvatochromic plots and those from IEOEM. We should discuss the origin of the solvent dependence of dipole moments derived from the solvatochromic plots and from IEOEM.

According to eq 1, if it is assumed that the entire solvent dependence of $\boldsymbol{\mu}_e$ should be recognized as an induced part through the term $\alpha\boldsymbol{R}$ as the function of the solvent polarity, then eq 1 can be further reduced with respect to $\boldsymbol{\mu}_e$:

$$\frac{1}{\boldsymbol{\mu}_e} = \frac{1}{\boldsymbol{\mu}_e^0}\left[1 - \frac{\alpha}{2\pi\epsilon_0 {a_0}^3}\frac{\epsilon - 1}{2\epsilon + 1}\right] \qquad (15)$$

This equation implies that plots of the obtained values of $1/|\boldsymbol{\mu}_e|$ versus $(\epsilon - 1)/(2\epsilon + 1)$ would yield a straight line, then the polarization density $\alpha/{a_0}^3$ can be derived from the slope.

In a previous paper,[4] Baumann et al. reported the plot of $1/|\boldsymbol{\mu}_e|$ for **BA** versus $(\epsilon - 1)/(2\epsilon + 1)$ with 22 solvents of different ϵ, by means of EOEM and IEOEM. They analyzed the plot assuming the linear dependence by eq 15 to obtain $\boldsymbol{\mu}_e$ and α. The plots for **3A**, **3H**, and **2B** obtained by IEOEM in this work are given in Figure 9. In the present case only three solvents were used, but the plots do not seem to deviate largely from the straight line. Similar relations were also observed for other anthrylenes investigated here. Based on the slope of the plot, the estimated values of $\alpha/{a_0}^3$ are summarized in Table 2. The calculated values for $\alpha/{a_0}^3$ have been found to be very large compared to those for common hydrocarbons or aromatic compounds and almost equal to that of a conducting sphere.[4]

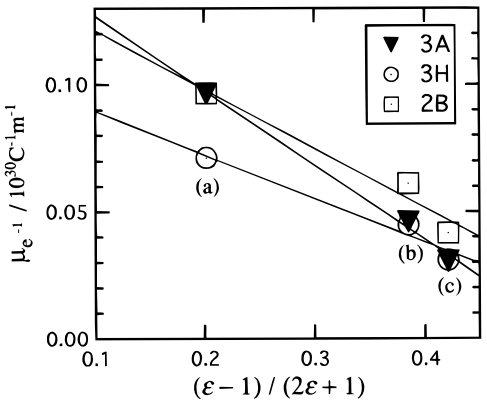

Figure 9. Plots of the inverse of the dipole moment $1/|\boldsymbol{\mu}_e|$ of **3A** (triangles), **3H** (circles), and **2B** (squares) against the function of the relative permittivity of the solvent $(\epsilon - 1)/(2\epsilon + 1)$ according to eq 15. Solvents used are cyclohexane (a), dioxane (b), and trifluorotoluene (c). The lines correspond to the best fit straight line through the cyclohexane value.

TABLE 3: Fluorescence Spectral Band Dependences of $\boldsymbol{\mu}_e$ of 3A, 3H, and 2B in Trifluorotoluene Observed by IEOEM

compounds	$\boldsymbol{\mu}_e$/D (cutoff wavelength/nm)[a]		
3A	9.8(380[b])	9.9(450)	9.8(470)
3H	9.0(380)	8.6(450)	8.7(490)
2B	7.2(380)	7.2(423)	7.3(450)

[a] Type of the cutoff filter in order to eliminate contribution from the emission band at the shorter wavelength region. The filter was positioned in front of the detecting photomultiplier. [b] The filter of 380 nm cutoff was employed to avoid UV scatters from the high-pressure mercury lamp used as the excitation source. The emission bands of the anthrylenes were observed in the region longer than 380 nm in trifluorotoluene.

The polarizability volume $\alpha' (=\alpha/4\pi\epsilon_0) = 220 \times 10^{-24}$ cm^3 is derived for **BA** by using $a_0 = 6$ Å, for instance, while α' for anthracene along the short axis of the molecule is $(30 \pm 3) \times 10^{-24}$ cm^3 in the ground state and $(36 \pm 6) \times 10^{-24}$ cm^3 in the excited state, respectively, according to the literature.[26] For other anthrylenes, the estimated values of α' are given in Table 2, which were derived under the two different assumptions of a_0 as described in the preceding section. Note that especially for the trimers the values of α' are even much larger as compared to that of **BA**. These results are, in part, due to the assumption that the entire part of the solvent dependence of $\boldsymbol{\mu}_e$ is of solvent induced origin, through the term $\alpha\boldsymbol{R}$ in eq 1.

We then have attempted to detect the effects of the contribution from the excitonic state to the CS state; several cutoff filters for the shorter wavelength region were set in front of the photomultiplier and IEOEM were performed for **3A**, **3H**, and **2B** in trifluorotoluene. Obtained dipole moments are summarized in Table 3. Any significant differences were not detected. This result indicates that the smaller values of $\boldsymbol{\mu}_e$ for **2B** (and also for **3B**, speculatively) in trifluorotoluene should not be interpreted as a consequence of an interference from smaller excitonic dipole moments.

To estimate $\boldsymbol{\mu}_e$ from the solvatochromic plots, a suitable assumption of a_0 must be necessary. In the present calculation, two different a_0 were employed, and both assumptions should be acceptable. However, even smaller results of $\boldsymbol{\mu}_e$ estimated from the solvatochromic plots based on the shorter choices a_0 are relatively larger compared to those from IEOEM.

In the present work the slope of the solvatochromic plot was determined from the higher polarity region of the abscissa as given in Figure 3, and the plots actually can be regarded as

straight lines in this region. Note that $f_\epsilon - (1/2)f_n \approx 0.284$, 0.293, 0.323, and 0.378 for the representative solvents used in this work corresponding to dioxane, ethyl acetate, trifluorotoluene, and DMF, respectively. In the present solvatochromic plots the parameter $f_\epsilon - (1/2)f_n$ was adopted as the abscissa, where it was assumed that dipole moments other than $\boldsymbol{\mu}_e$ could be neglected. In the previous papers we reported the transient absorption spectra of **BA**[9] and **3H**[11] in polar solvents, by means of a femtosecond−picosecond spectroscopy. The results showed that at just after the laser excitation the transient absorption spectra of **BA** and **3H** were essentially equal to the $S_n \leftarrow S_1$ absorption spectra of the corresponding anthryl monomers. With time evolution, the spectra had gradually changed to those assigned to be the CS state, within a few picoseconds. Similar results with respect to the spectral evolution were also observed for **2B** and **3B**.[27] These experimental results also support the assumption for the derivation of eqs 6 and 7, which are originated from eq 4, with respect to the abscissa, $f_\epsilon - (1/2)f_n$, used in the present solvatochromic plots. Unsuitable estimations of the slope of the solvatochromic plots might not be responsible for the discrepancies of $\boldsymbol{\mu}_e$.

Then the linear regressions of $\tilde{\nu}$ against $f_\epsilon - (1/2)f_n$ can be interpreted as the variation of the reaction field due to the change of the solvent polarity, while $\boldsymbol{\mu}_e$ is assumed to be constant. On the other hand, as shown in Figures 4−7 the transient absorption spectra of the anthrylenes drastically change from excitonic-like states toward CS states as the solvent polarity increases. It is stressed here that $\boldsymbol{\mu}_e$ estimated by means of the solvatochromic plots based on eq 7 in this work can be explained as a dipole moment that is averaged over the solvent polarity region from which the slope of the plot is determined. The situation is even similar for the present interpretation of the result from IEOEM. As stated previously, the CS state of the present anthrylenes is not a one-electron-transfer state even in the polar solvents acetonitrile and DMF but is a partial CS state that can be expressed by a notation like $A^{\delta+}-A^{\delta-}$. On the other hand, solvent polarity effects on the transient absorption spectra should be mainly ascribed to an electronic structure change due to solute−solvent interaction. It is considered that the larger $\boldsymbol{\mu}_e$ of the anthrylenes as observable from two experimental methods should therefore be corresponding to larger $\delta+$ and $\delta-$, which then cannot simply be interpreted by electronic polarizability induced origin. This substantial electronic structure change of the solute could cause changes of $\boldsymbol{\mu}_e$. Then the simple theory of fluorescence solvatochromic plots or of IEOEM for a sufficiently rigid molecule must fail since $\boldsymbol{\mu}_e$ is assumed to be constant in the underlying methods.

We also investigated the solvent dependence of the electronic structure of **3C** as a reference compound as well as other anthrylenes. Steady-state and transient spectroscopy has revealed that **3C** forms a CS state even in the nonpolar solvent, and the charge-transfer interaction between cyanoanthracene and the remaining part of **3C** is much stronger than that of other anthrylenes. For **3C** $\boldsymbol{\mu}_e$ estimated from the solvatochromic plot and IEOEM are also shown in Tables 1 and 2, respectively. In this case the absolute values of $\boldsymbol{\mu}_e$ actually seem to be rather compatible to each other, reflecting a smaller effect of the solvent-induced change of the electronic structure on $\boldsymbol{\mu}_e$ compared to other anthrylenes. Alternatively stated, the significant deviation of $\boldsymbol{\mu}_e$ should be characteristic for the solute of which the electronic structure in the excited state can be substantially affected by the solute−solvent interaction. A similar result of the solvent effects on $\boldsymbol{\mu}_e$ and solvatochromic shifts was reported in the case of 4-(9-anthryl)-*N*,*N*-dimethylaniline where the charge-transfer interaction in both ground and excited states is more effective compared to the case of **3C**.[28] On the other hand, even in the case of **3C** where the relative compatibility of $\boldsymbol{\mu}_e$ was observed, the calculated α' still has an extraordinary large value. This result implies that the solvent-induced change of the electronic structure should be considerable also for **3C**.

In the present case, the electronic structures of the anthrylenes have been approximated as point dipole moments irrespective of the geometry change in their excited states, and contributions from higher multipole moments have been neglected. In relation to the validity of the approximation used here, Sato and Kato have provided potential energy of dipoler molecules in solution by means of the image approximation and applied the calculations to two sample reactions, tautomeric proton transfer and S_N2 reactions.[29] Their work may imply that if we used some elaborated theoretical models including multipole terms for the analysis of dipole moments, the estimated values of $\boldsymbol{\mu}_e$ would hardly deviate from the present results. In this work, both theoretical frameworks of the solvatochromic plot and IEOEM rely basically on energetics of the concerned electronic states, assuming point dipole moments located on the center of a sphere.

More precise quantum chemical treatments for the mechanisms of the solvent effects on the electronic state have been made by Kato et al.[30,31] They constructed the free energy potential surface of 4-(*N*,*N*-dimethylamino)benzonitrile in polar solvents for the elucidation of the formation mechanism of a TICT state that is coupled with the rotation of the dimethylamino group and the solvation dynamics. Hirata and Kato et al.[32−34] have studied solvent effects on some chemical reaction dynamics on the basis of the reference interaction site model. A specific theoretical approach also for the system of present anthrylenes is highly desirable.

Lower Possibility of the CS State for the *tert*-Butyl-Substituted Anthrylenes: 2B and 3B. A prominent experimental result from the present work is that *tert*-butyl-substituted **2B** and **3B** exhibit a lower possibility of achieving the CS state, whereas the other oligomers **3A** and **3H** show characteristics of the CS state similar to those of **BA** as described above. It is also indicated that apart from the discrepancy of $\boldsymbol{\mu}_e$ determined by the different experimental methods, the $\boldsymbol{\mu}_e$ for **2B** and **3B** is estimated to be smaller than those of the other compounds, as indicated by both the solvatochromic plots and IEOEM. Availability of the CS state is largely controlled by the substituent group rather than the number of the anthrylene chains.

As described in the Results section, the steady-state absorption and fluorescence spectra and the $S_n \leftarrow S_1$ absorption spectrum of 2,6-di-*tert*-butylanthracene are just in agreement with those of anthracene. In addition, the cationic and anionic radical absorption spectra of 2,6-di-*tert*-butylanthracene were also very similar to their corresponding species of anthracene. In the same way, the steady-state absorption and fluorescence spectra and the $S_n \leftarrow S_1$ and ionic absorption spectra of 2,3-dihexylanthracene are also very similar to those of anthracene.[11] *tert*-Butyl as well as *n*-hexyl[11] groups would hardly affect the electronic structure of anthracene in its ground and excited states. The possibility of the CS state should be discussed from a viewpoint other than the electronic structure of the corresponding anthryl monomers.

In solution, a dipole moment located in an empty sphere can be energetically stabilized, and the stabilization energy can be obtained by Onsager's equation. For **2B** and **3B**, due to the

bulky *tert*-butyl substituents, the solvation radii might be larger compared to other anthrylenes. The larger effective Onsager cavity could give rise to a smaller solvation energy. According to the molecular weight model as given in Table 1, $a_0 = 6.8$ Å was assumed for **3A** and $a_0 = 7.5$ Å for **3B**. We may evaluate the energy of the CS state of **3B** with a dipole moment equal to that of **3A**, 21 D, by the aid of the result of the solvatochromic plots of **3A** (Table 1). In Figure 3, the energy of the CS state of **3A** seems to be equal to that of the excitonic state around $f_\epsilon - (1/2)f_n \approx 0.20-0.25$ where the fluorescence of the CS state was actually observed. The dotted line with milder slope in Figure 3 indicates the hypothetically estimated energy difference between the equilibrated ground state and the CS state with 21 D of **3B**. On the other hand, the dot−dashed and dot−dot−dashed lines in Figure 3 show the emission from the excitonic state of **3A** and **3B**, respectively. This estimation has predicted that the hypothetical CS sate of **3B** might decrease the solvation energy about 700 cm^{-1} (0.087 eV) in the solvent DMF where $f_\epsilon - (1/2)f_n = 0.378$, for example.

Actually, this simple calculation may overestimate the solvation energy of the CS state of **3B**. As described in the Results section, a major part of the transient absorption spectrum of **3A** in ethyl acetate (Figure 4a) is ascribed to the excitonic state, while a rather small contribution from the CS state is recognized especially in the longer wavelength region (>650 nm). Then such an assumption may also be appropriate that the CS state of **3A** would be possible in the solvents more polar than ethyl acetate. In this case, the dotted line in Figure 3 shifts rightward and crosses around $f_\epsilon - (1/2)f_n \approx 0.29$ (ethyl acetate).

Having the above discussion in mind, we can thus consider that after the excitation, there should exist the two possible pathways to reach an equilibrated excited state: one is to the excitonic state and another is to the CS state. For **BA**, **3A**, and **3H**, the energetically favorable CS state should be predominant in polar solvents. In the case of **2B** and **3B**, on the other hand, because of the smaller solvation energy they relax into the excitonic-like state even in polar solvents. For **3H**, it might be possible that two *n*-hexyl groups also hinder the solvation. However, the *n*-hexyl groups are flexible and are attached to the mother anthrylene part by only the 2″ and 3″ sites of the central anthryl moiety, and the remaining sites could be solvated like **BA** and **3A**. This is a plausible explanation for less availability of the CS state for **2B** and **3B**.

It should be noted here that in the present study acetonitrile and DMF were employed as a common high-polarity and nonviscous solvent, with $\epsilon = 37.5$ and the viscosity $\eta = 0.36$ cP for acetonitrile, and $\epsilon = 36.7$ and $\eta = 0.80$ cP for DMF, respectively. In *N*-methylformamide (NMF) with much higher polarity ($\epsilon = 182$) and viscosity ($\eta = 1.65$ cP), **2B** and **3B** indicate larger Stokes shifts than those in DMF,[27] with the fluorescence maxima at 472 nm (21.2×10^3 cm^{-1}) for **2B** and 461 nm (21.7×10^3 cm^{-1}; see also Figure 3) for **3B**. The transient absorption spectrum of **2B** in NMF in the equilibrated excited state is just very similar to that of **BA** in NMF. In NMF with the strongest polarity, despite their larger solvation radii, the *tert*-butyl-substituted anthrylenes may well achieve a similar CS state compared to the other anthrylenes. Details on the formation of the CS state of **2B** and **3B** in NMF will be discussed in our forthcoming paper.[27]

For the present anthrylenes, in the ground state the anthrylene chromophores are considered to be distributed around the perpendicular conformation irrespective of the substituents, while in the excitonic state the chromophores have the twisted form. It is considered that the relative conformation between the anthrylene chromophores has a close coupling to the electronic structure in the excited states. Wortmann et al.[8] actually estimated the solvent dependence of the effective torsional potential of **BA** extracted from the band-shape analysis on the steady-state fluorescence spectra and found that in nonpolar/slightly polar solvents the S_1 potential minimum shifts a little toward a more twisted conformation, as the solvent polarity increases. On the other hand, to achieve CS states an appropriate intramolecular rotational relaxation around the single bond(s) that connect(s) the anthrylene chromophores seems to be necessary.

TABLE 4: Intramolecular Geometrical Relaxation Times τ in Cyclohexane

	τ/ps[a]
BA[b]	10
3H[c]	11
2B	12
3B	10

[a] Estimated by the analysis of spectral time evolution of transient absorption from the $S_n \leftarrow S_1$ spectra of the corresponding anthrylene monomers to the relaxed excitonic states. [b] Taken from ref 7. [c] Taken from ref 11.

In previous papers we reported the geometrical relaxation times τ of **BA**[7] and **3H**[11] in cyclohexane by means of subpicosecond transient absorption spectroscopy. We have actually observed that the transient absorption spectra of **2B** and **3B** in cyclohexane change from the $S_n \leftarrow S_1$ absorption spectra of 2,6-di-*tert*-butylanthracene at just after the excitation toward the relaxed excitonic state, like in the case of **BA** or **3H**. We parenthetically note that such a measurement of **3A** could not be achieved due to poor solubility. As listed in Table 4, values of τ estimated from the spectral evolution are clustered around ≈10 ps, and this value is independent of the specific anthrylene structure. This result implies that with even bulky *tert*-butyl substituent groups the dynamics of **2B** and **3B** with respect to the conformational relaxation should be comparable with those of **BA** and **3H**. In other words, lower possibility of the CS states for **2B** and **3B** could not be attributed to the intramolecular relaxation dynamics around the single bond(s). For less CS in the case of **2B** and **3B** even in polar solvents an explanation based on the static energetics, as described before, could instead be more reasonable.

Conclusions

In this work we have investigated the solvent-induced changes of the electronic structure of the 9,10-anthrylene dimers and trimers analogous to 9,9′-bianthryl (**BA**). Steady-state absorption and fluorescence spectroscopy and transient absorption spectra measurements have been applied for the elucidation of the possibility of the charge separation (CS) in the excited state. The dipole moments of the anthrylenes in the equilibrated excited state $\boldsymbol{\mu}_e$ have been determined by the solvatochromic fluorescence shifts, as well as integrated electrooptical emission measurements (IEOEM). The CS state is strongly controlled by the substituent group introduced upon the anthrylene skeleton. Both unsubstituted and *n*-hexyl-substituted trimers, **3A** and **3H**, respectively, indicate very similar behavior compared to BA. On the other hand, the *tert*-butyl-substituted dimer (**2B**) and trimer (**3B**) show lower possibility of the CS state even in polar solvents such as DMF. Less availability of the CS state for the *tert*-butyl-substituted compounds has been mainly ascribed to their smaller solvation energy due to their larger effective Onsager radii. At the present stage of our investigation, an explanation based on the relaxation dynamics of intramolecular

rotation around the single bond(s) connecting the anthryl moieties cannot be applicable for less CS for **2B** and **3B**. From the dipole moment measurements, larger μ_e values have been obtained for **BA**, **3A**, and **3H**, while much smaller values have been observed for **2B** and **3B**. Despite the qualitative agreement of the tendency of μ_e determined from the different two methods, the values of μ_e estimated from the solvatochromic plots were much larger compared to those obtained by IEOEM. It has been confirmed that such a simple model for the solvatochromic plots or IEOEM that the entire part of the solvent dependence of μ_e is interpreted by the electronic polarizability origin not being applicable for the present anthrylenes, the main reason being structural changes other than purely electronic (e.g., twist angles). The discrepancy of μ_e determined from the above-mentioned two methods should thus be characteristic for the present anthrylenes, where the solvent-induced electronic structure change plays a substantial role.

Acknowledgment. We thank Dr. T. Magnel of Max-Planck-Institut for the preparation of **3A**. T.O. and W.B. acknowledge the support by the Grant-in-Aid for the International Scientific Research Program−Joint Research (No. 05044055) from the Ministry of Education, Science, Sports and Culture of Japan.

References and Notes

(1) Schneider, V. F.; Lippert, E. *Ber. Bunsen-Ges. Phys. Chem.* **1968**, *72*, 1155.

(2) Nakashima, N.; Murakawa, M.; Mataga, N. *Bull. Chem. Soc. Jpn.* **1976**, *49*, 854.

(3) Rettig, W.; Zander, M. *Ber. Bunsen-Ges. Phys. Chem.* **1983**, *87*, 1143.

(4) Baumann, W.; Spohr, E.; Bischof, H.; Liptay, W. *J. Lumin.* **1987**, *37*, 227.

(5) Kang, T. J.; Kahlow, M. A.; Giser, D.; Swallen, S.; Nagarajan, V.; Jarzeba, W.; Barbara, P. F. *J. Phys. Chem.* **1988**, *92*, 6800.

(6) Mataga, N.; Yao, H.; Okada, T.; Rettig, W. *J. Phys. Chem.* **1989**, *93*, 3383.

(7) Okada, T.; Nishikawa, S.; Kanaji, K.; Mataga, N. In *Ultrafast Phenomena VII*; Harris, C. B., Ippen, E. P., Mourou, G. A., Zweil, A. H., Eds.; Springer-Verlag: Berlin, 1990; p 397.

(8) Wortmann, R.; Lebus, S.; Elich, K.; Assar, S.; Detzer, N.; Liptay, W. *Chem. Phys. Lett.* **1992**, *198*, 220.

(9) Mataga, N.; Nishikawa, S.; Okada, T. *Chem. Phys. Lett.* **1996**, *257*, 327.

(10) Elich, K.; Kitazawa, M.; Okada, T.; Wortmann, W. *J. Phys. Chem. A* **1997**, *101*, 2010.

(11) Fritz, R.; Rettig, W.; Nishiyama, K.; Okada, T.; Müller, U.; Müllen, K. *J. Phys. Chem. A* **1997**, *101*, 2796.

(12) Onsager, L. *J. Am. Chem. Sci.* **1936**, *58*, 1486.

(13) Baumann, W. In *Physical Methods of Chemistry*; Rossiter, B. W., Hamilton, J. F., Eds; John Wiley and Sons: New York, 1989; Vol. III, Part B, Chapter 2.

(14) Mataga, N.; Kaifu, Y.; Koizumi, M. *Bull. Chem. Soc. Jpn.* **1955**, *28*, 690.

(15) Lippert, E. *Z. Naturforsch.* **1955**, *10a*, 541.

(16) Mataga, N.; Kubota, T. In *Molecular Interactions and Electronic Spectra*; Marcel Dekker: New York, 1970; Chapter 8.

(17) Liptay, W. In *Excited States*; Academic Press: New York, 1974; Vol. 1, p 129.

(18) Baumann, W.; Nagy, Z.; Maiti, A. K.; Reis, H.; Rodrigues, S. V.; Detzer, N. In *Dynamics and Mechanisms of Photoinduced Electron Transfer and Related Phenomena*; Mataga, N., Okada, T., Masuhara, H., Eds.; Elsevier: Amsterdam, 1992; p 211.

(19) Baumann, W.; Deckers, H. *Ber. Bunsen-Ges. Phys. Chem.* **1977**, *81*, 786.

(20) Deckers, H.; Baumann, W. *Ber. Bunsen-Ges. Phys. Chem.* **1977**, *81*, 795.

(21) Hirata, Y.; Okada, T.; Mataga, N.; Nomoto, T. *J. Phys. Chem.* **1992**, *96*, 6559.

(22) Müller, U.; Adam, M.; Müllen, K. *Chem. Ber.* **1994**, *127*, 437.

(23) Kahlow, M. A.; Kang, T. J.; Barbara, P. F. *J. Chem. Phys.* **1988**, *88*, 2372.

(24) Horng, M. L.; Gardecki, J. A.; Papazyan, A.; Maroncelli, M. *J. Phys. Chem.* **1995**, *99*, 17311.

(25) Yao, H.; Okada, T.; Mataga, N., unpublished results.

(26) Liptay, W.; Walz, G.; Baumann, W.; Schlosser, H.-J.; Deckers, H.; Detzer, N. *Z. Naturforsch* **1971**, *26a*, 2020.

(27) Nishiyama, K.; Honda, T.; Okada, T.; Müllen, K., manuscript in preparation.

(28) Baumann, W.; Petzke, F.; Loosen, K.-D. *Z. Naturforsch.* **1979**, *34a*, 1072.

(29) Sato, H.; Kato, S. *J. Mol. Struct. (THEOCHEM)* **1994**, *310*, 67.

(30) Kato, S.; Amatatsu, Y. *J. Chem. Phys.* **1990**, *92*, 7241.

(31) Hayashi, S.; Ando, K.; Kato, S. *J. Phys. Chem.* **1995**, *99*, 955.

(32) Ten-no, S.; Hirata, F.; Kato, S. *J. Chem. Phys.* **1994**, *100*, 7443.

(33) Sato, H.; Hirata, F.; Kato, S. *J. Chem. Phys.* **1996**, *105*, 1546.

(34) Kawata, M.; Ten-no, S.; Kato, S.; Hirata, F. *J. Phys. Chem.* **1996**, *100*, 1111.